

This article was downloaded by: [Siauliu University Library]

On: 17 February 2013, At: 07:17

Publisher: Taylor & Francis

Informa Ltd Registered in England and Wales Registered Number: 1072954 Registered office: Mortimer House, 37-41 Mortimer Street, London W1T 3JH, UK



Advanced Composite Materials

Publication details, including instructions for authors and subscription information:

<http://www.tandfonline.com/loi/tacm20>

Instability of thin composite isogrid panel during autoclave cure cycle

Thomas D. Kim

Version of record first published: 02 Apr 2012.

To cite this article: Thomas D. Kim (2000): Instability of thin composite isogrid panel during autoclave cure cycle, *Advanced Composite Materials*, 9:2, 119-130

To link to this article: <http://dx.doi.org/10.1163/15685510051029255>

PLEASE SCROLL DOWN FOR ARTICLE

Full terms and conditions of use: <http://www.tandfonline.com/page/terms-and-conditions>

This article may be used for research, teaching, and private study purposes. Any substantial or systematic reproduction, redistribution, reselling, loan, sub-licensing, systematic supply, or distribution in any form to anyone is expressly forbidden.

The publisher does not give any warranty express or implied or make any representation that the contents will be complete or accurate or up to date. The accuracy of any instructions, formulae, and drug doses should be independently verified with primary sources. The publisher shall not be liable for any loss, actions, claims, proceedings, demand, or costs or damages whatsoever or howsoever caused arising directly or indirectly in connection with or arising out of the use of this material.

Instability of thin composite isogrid panel during autoclave cure cycle

THOMAS D. KIM¹ and CHRISTOPHER A. ROTZ²

¹ *Asian Office of Aerospace Research and Development, 7-23-17 Roppongi, Minato-ku, Tokyo, 106-0032, Japan*

² *Brigham Young University, Department of Manufacturing and Engineering Technology, Provo, Utah 84602, USA*

Received 14 July 1999; accepted 20 October 1999

Abstract—This paper describes the analyses performed to determine why nominally flat composite isogrid panels designed for the Clementine I satellite were warping during the autoclave cure cycle. Analytical models indicated that the largest factor was the mismatch in the coefficient of thermal expansion of different parts of the tooling. The next most important factor was the coefficient of thermal expansion mismatch between the skin and rib materials of the composite isogrid itself. A new tooling design eliminated the first factor, producing a rib-only panel with no warping. An analytical model was developed, which predicted that warping caused by the rib/skin mismatch would be 3.31 mm over a length of 147.32 cm. A panel with the skin was manufactured and found to have a warp of 3.80 mm. Further improvements in producing flat panels will depend on finding appropriate materials for the rib and skin.

Keywords: Composite; isogrid; autoclave; warping; substrate; interferometer; modeling; Clementine.

1. INTRODUCTION

The development of highly efficient structures, such as the composite isogrid stiffened structure, promises to improve the next generation of aerospace components. One space component that can greatly benefit from the composite isogrid structure is the solar array substrate panel. Most current rigid solar array substrates are fabricated from the aluminum honeycomb with graphite epoxy face sheets [1]. However, isogrid panels provided greater stiffness for a given weight compared with equivalent honeycomb sandwich structures. Also, unlike honeycomb structures, isogrid structures have no middle ‘core’ that could hinder heat flux through the depth of the panel. Therefore, the temperature difference (ΔT) of the isogrid panel is much smaller than that of the honeycomb panel. Additionally, the back surface of the isogrid is stiffened rather than flat. This provides an increased surface area to dissipate

heat or functions as a heat dissipating fin. Solar cells benefit from this by operating at lower temperature, which generates higher cell efficiency.

Realizing many potentials, the Air Force Research Laboratory has successfully manufactured flat isogrid panels approximately 61.0 cm by 61.0 cm in size [2, 3]. Upon successful development of small isogrid panels, the Laboratory began a six month project to design, fabricate and test composite isogrid solar array panels (91 cm by 152 cm) for the Clementine spacecraft as shown in Fig. 1. The intention was to produce a design that would have at least equivalent in-plane stiffness, bending stiffness, and thickness as the current aluminum honeycomb design while reducing the weight. To this end, an isogrid configuration was chosen because of its damage tolerance and buckle resistant characteristics [4–6].

Using the graphite/epoxy (IM7/977-2) material and advanced processing technique, efforts were started to fabricate the 91 cm by 152 cm substrate with a skin thickness of 0.38 mm, rib thickness and depth of 1.52 mm and 12.32 mm, respectively. This substrate design had an in-plane and bending stiffness of 38 153 N/m and 1 023 N/m, respectively. These values resulted in a natural frequency of ap-

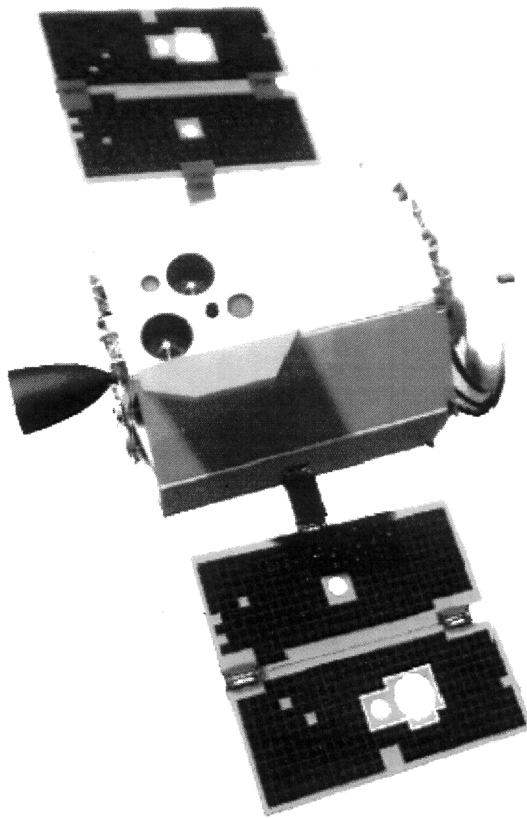


Figure 1. Clementine I spacecraft.

proximately 60 Hz, well in excess of the 30 Hz required. The total weight of the panel was 1.35 kg.

The composite isogrid design met or exceeded all requirements for strength, stiffness, and interfaces except for one: the solar cell integrator requirement that the surface be flat within 0.76 mm over its total length. This was not thought to be a problem since the small panels had met this constraint. Unfortunately, the first autoclaved cured panels were not flat; some had bows of 10.16 mm. The flatness requirement became a major obstacle during the fabrication process. Several changes in materials and tooling were tried and some improvements were made, but none was successful in meeting the flatness requirement. The purposes of this project were to determine the causes of the warping and to devise a method for producing flat panels within the tolerances required by the Clementine program office. This paper will present a summary of the theoretical and experimental work done to understand the problem, a proposed method for manufacturing flat panels, and the experimental work done to verify the proposed solution.

2. BACKGROUND

The first step in this project was to gather all available information on the prior attempts to manufacture the large isogrid substrates as shown in Fig. 2. It was hoped that some conclusions about the causes of the warping could be drawn once the data were organized and examined.

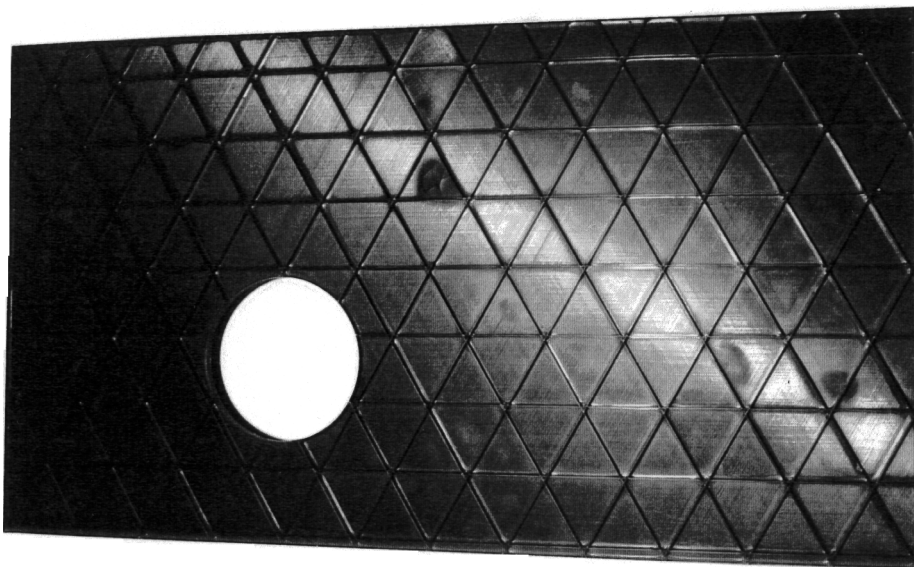


Figure 2. Clementine solar array substrate.

2.1. Basic isogrid tooling

The geometry of the basic isogrid concept is shown in Fig. 3, and Fig. 4 shows some important dimensions for the rib/skin design. Figure 5 shows the basic setup for fabricating small isogrid panels. The mold was made from RTV silicone rubber, which was placed on top of the 12.7 mm thick steel base plate with borders to constrain the rubber from expanding. There was a 6.3 mm expansion gap between the border and the mold.

Winding prepreg tow into isogrid shaped slots in the silicone rubber mold formed the ribs. Between 35 to 40 layups are needed to fill the 12.7 mm deep slots by stacking the tow fibers on top of each other until the slot was filled to the top. Spreading the fibers offset the buildup at the nodes. Prepreg tape was laid over the mold and ribs to form the skin. The 12.7 mm thick caul plate was placed on top of the skin to get a compaction. The entire part was bagged and cured in an autoclave.

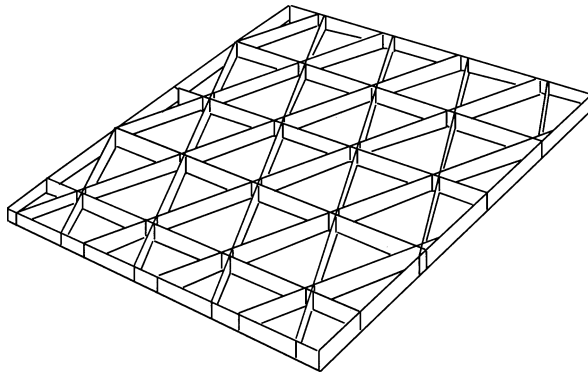


Figure 3. Isogrid stiffened panel.

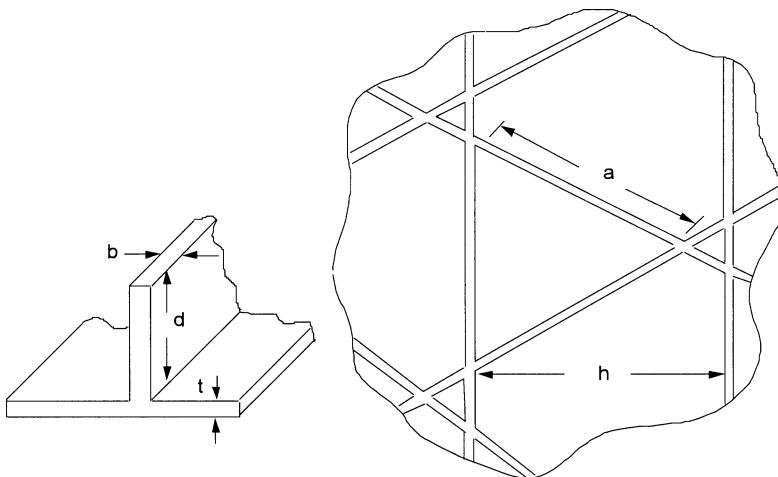


Figure 4. Geometry for the isogrid panel: the dimensions were: $t = 0.38$ mm, $d = 12.32$ mm, $b = 1.52$ mm, $h = 82.55$ mm, $a = 95.76$ mm.

2.2. Substrate tooling

Alternate tooling systems used for fabricating Clementine panels are shown in Fig. 6. The barrier-frame setup was similar to the original tooling, except that the steel barriers were replaced by a frame made from steel bars ($6.3 \text{ mm} \times 34.99 \text{ mm}$ in cross-section) and the base plate was made from 12.7 mm thick K100 tooling material. The bars were pinned together but were not attached to the base plate. The frame fit snugly against the rubber mold. The unconstrained rubber mold and the loose borders could have contributed to the warping. A summary of the materials and lay-up sequences used to fabricate the prior panels is shown in Table 1.

The isogrids were all made from carbon fiber reinforced epoxy (977-2) or dicyanate ester (DCE) in the form of prepreg tow and unidirectional tape. The fibers were either IM7 or P75 purchased from the Fiberite company. In some cases, panels were fabricated without skins. In all cases, a release sheet was placed between the skin and the caul plate, and the tooling was completely enclosed in a vacuum bag. All curing was done in an autoclave for 2 h at 177°C and a pressure of 0.552 MPa.

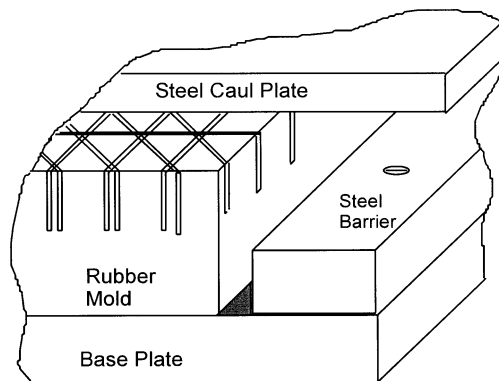


Figure 5. Diagram of basic tooling.

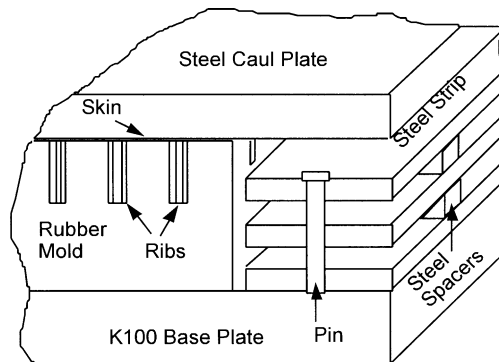


Figure 6. Alternative tooling concept.

Table 1.
Warping results of previously fabricated isogrid panels

Part number	Rib material	Rib stacking (0°)	Skin material	Skin layup	Measured warping (mm)
1	IM7 DCE	39 tows	P75 DCE	6 Plies (±60,0)	7.89
2	IM7 977-2	39 tows	IM7 977-2	4 Plies (90,0)	16.3
3	IM7 977-2	42 tows	IM7 977-2	4 Plies (90,0)	6.30
4	IM7 DCE	57 tows	IM7 DCE	3Plies (±60,0)	N/A

3. CAUSES OF WARPING

A ribs-only panel was studied in more detail by mapping out its warping, as shown in Fig. 7. The panel was placed on a precision flat granite slab, and the distances from the slab surface to the tops of the ribs were measured with a depth micrometer. The rib height (dimension *d* in Fig. 4) was subtracted, leaving the warping distance as the result. The data were then input to the contour plot generator of MATLAB [7]. The results showed maximum warping of 11.9 mm at the center of the panel.

It was difficult to draw any firm conclusions from the warping results for the panels. Too many variables were changed from one attempt to the next to determine exact cause and effect relationships. Some of the critical data that might make such an assessment possible are missing, such as the thermal-couple reading of the entire tooling and composite part during the cure cycle. Even though available data do not conclusively identify the cause of the warping problem, the following seem to be the most likely explanations:

- Since the vacuum bag completely surrounds the tooling, it effectively forces the steel, rubber, and aluminum to move together in bending. Since these materials have different thermal expansion coefficients the tooling must therefore warp out of plane at elevated curing temperatures. The part was thus cured in a curved mold and retains its curved shape on returning to room temperature.
- The thermal expansion of the rubber was much higher than that of any other material used in the process and thus may cause warping as it cools, since it was not restrained on its sides during the cure cycle.
- The skin and rib materials have different thermal expansion coefficients and thus, even if the mold remains flat during cure, the part warps while returning to room temperature.
- Warping was caused by residual stresses in the parts due to nonuniform curing.

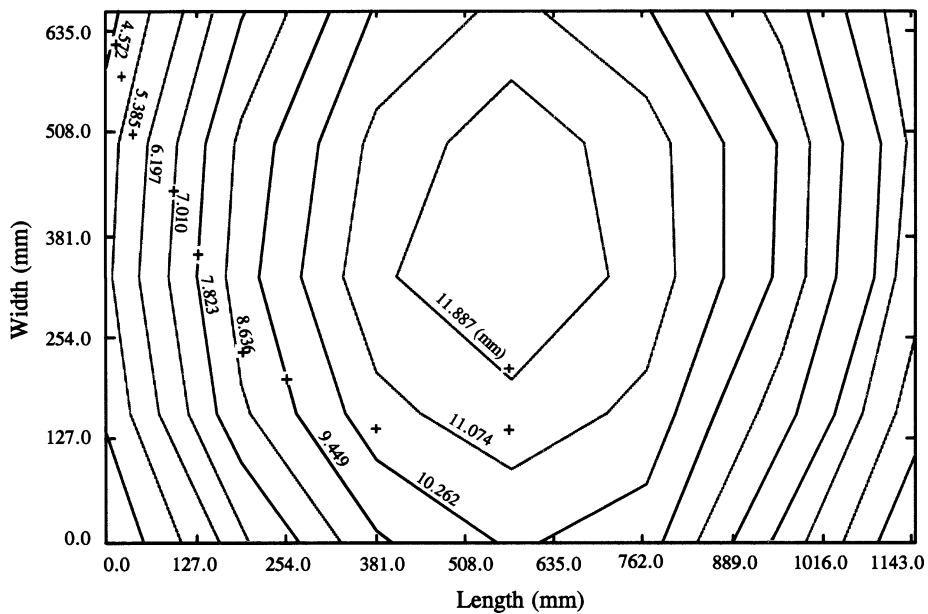


Figure 7. Contour plot of warped panel.

If the third explanation were the only cause of warping, then the ribs-only panels should have come out flat. Since it did not, it means that other causes must also be acting, and probably have a greater effect. The fourth explanation was tested by heating a ribs-only panel to 177°C in an oven. Since no change in its warped shape could be detected, it was concluded that residual stresses were not a major factor. It was postulated that warping of the panels comes from a combination of explanations 1, 2, and 3, and that either 1 or 2 are the dominant factors.

4. ANALYTICAL MODELING

Finite-element analysis of possible warping of the tooling during cure (explanation #1) was carried out for several different cases using PATRAN and Cosmic NAS-TRAN [8]. Since a vacuum bag completely surrounded the tooling and part during cure, the imposed 0.552 MPa autoclave pressure may have been high enough to prevent slip between the layers. Thus it was assumed that the tooling, ribs, and skin all deformed as a multilayer laminated plate under the thermal load imposed during cure [9].

The properties and dimensions of each layer in the model were the same as those of the actual parts, except for the rubber mold. The prepreg tows wound into the rib slots change the effective properties of the mold, so the mold was modeled as the two-layer laminate. The upper layer was assumed to have the properties of a quasi-isotropic fiber-reinforced composite material with a matrix of rubber and the

Table 2.
Properties used in the theoretical analysis

Properties	Materials				
	K100 aluminum	RTV rubber	Rubber and rib	Steel	Stainless steel
Thickness (mm)	12.7	25.4	12.7	12.7	1.524
Modulus (GPa)	68.9	1.03E-7	3.31E-6	209	193
Poisson's ratio	0.3	0.45	0.3	0.285	0.3
CTE (ppm/°C)	23.6	270.0	9.0	11.7	17.3

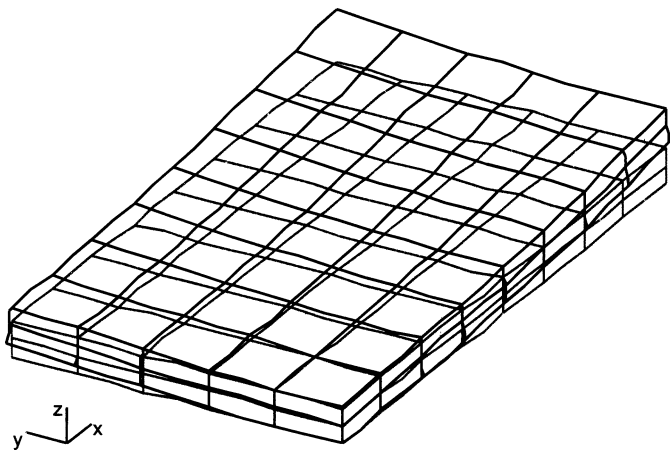


Figure 8. FEA model of deflected tooling.

tows acting as the fibers. (This layer is referred to hereafter as the ‘rubber and rib composite’). The bottom layer had the properties of the rubber alone.

The properties used in the analysis are listed in Table 2. For simplicity, all the layers were assumed to be 91.44 cm wide and 147.32 cm long. Because of symmetry in the set-up, only a quarter section of each laminated plate was modeled. The layers were divided into 20 node quadrilateral elements with 40 elements in each layer. A temperature load of 138°C was imposed in each case (21°C ambient temperature with a cure temperature of 177°C). Figure 8 shows NASTRAN result of the deflected shape, and Fig. 9 shows the contour plot of deflection. The results for the tooling plate show a maximum deflection of 2.04 mm.

The CTE values shown in Fig. 10 for the rubber and the composite materials were taken from data measured at Aerospace Corporation using the Michelson laser interferometer. The ribs were all uniaxial lay-ups while the skin was a six-ply laminate [+60, −60, 0, 0, −60, +60]. No four-ply data were available. Note that the

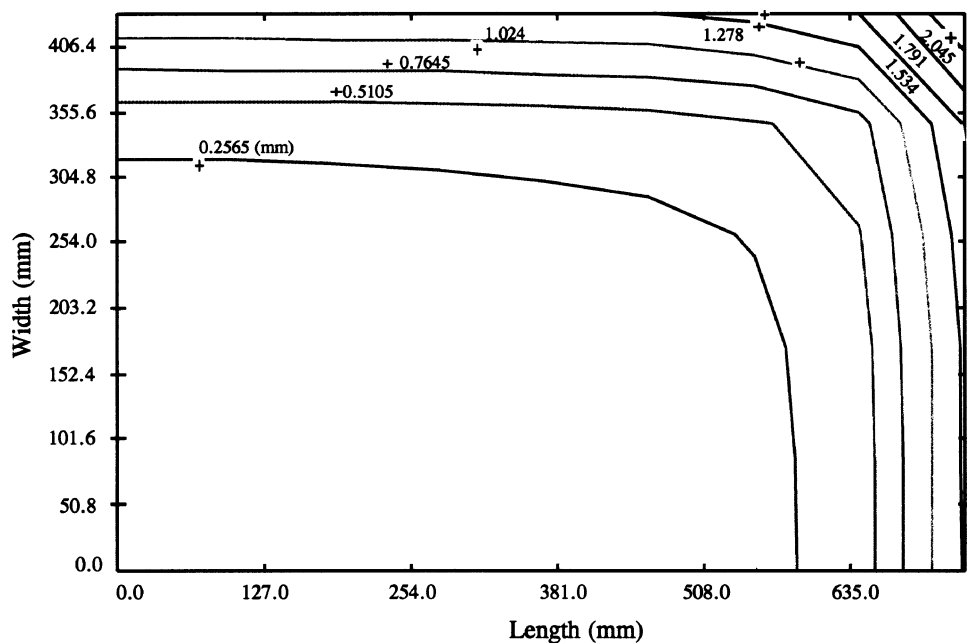


Figure 9. Contour plot of tool deflection.

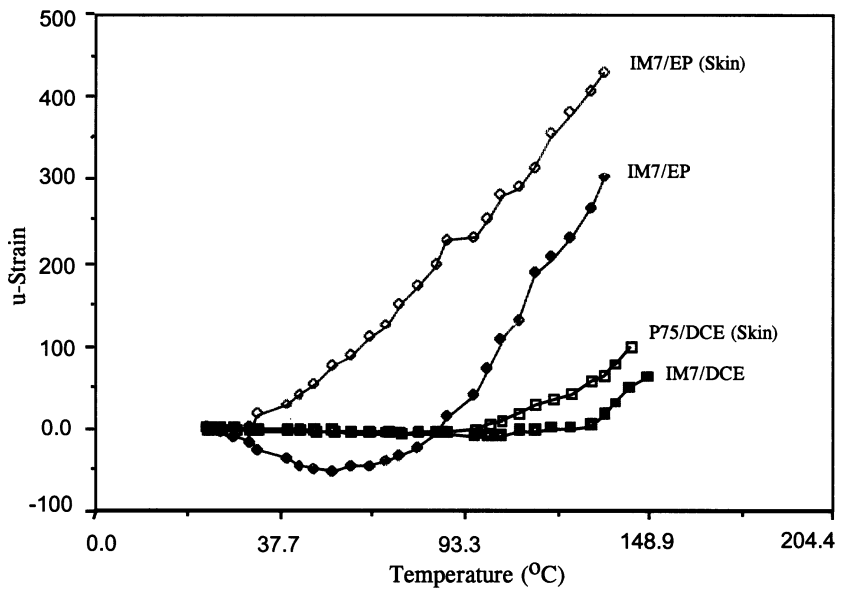


Figure 10. Coefficient of thermal expansion.

Table 3.
Predicted and actual panel warping

	Max panel deflection (mm)			
	1	2	3	4
Measured	7.87	16.26	6.35	9.14
FEA model	11.68	11.68	11.68	N/A
Beam model	0.0	9.65	9.65	10.41

slopes of the curves are not constant across the range of temperatures encountered during curing (21°C to 177°C). The data were extrapolated to 177°C and an effective secant CTE was used in all the calculations. Data for the silicone rubber are not shown, but its CTE value was $270.0 \times 10^{-6}/^{\circ}\text{C}$ compared to average CTE of $2.8 \times 10^{-6}/^{\circ}\text{C}$ for the composites. The analysis showed that amount of warping depends strongly on the difference between the CTE of the rib and that of the skin. For a panel made entirely of IM7/977-2 prepreg tape with six-ply skin, the predicted warping caused by this effect was 3.31 mm.

The tooling and part were also modeled as a laminated beam subjected to temperature loads. It was hoped that such a simple model would be useful for quick and easy estimating of the warping in the panels. A beam model could also be used to determine which of the design and tooling parameters had the greatest effects on warping. Equations for the bending deflections of such beams can be easily derived [10] and [11], so will not be repeated here. The appropriate beam equations were programmed into a spreadsheet, which was used for all the beam model calculations. Properties and dimensions used in the model were identical to those reported in the previous section. The theoretical predictions from the finite-element and beam models agree fairly well with the measured data as shown in Table 3. In a beam model it was assumed that plane sections remain plane during the deformation. Since the modulus of the rubber was so much smaller than that of the other materials used, this assumption may be invalid.

The beam model was used to study the effects of various parameters on the predicted warping. It was found that the biggest factor influencing warping was the difference in thermal expansion between the aluminum and steel tooling plates. The model also indicated that warping was much less sensitive to the properties of the rubber and the rubber-rib layer. Both models predict that, if steel plates are used, both top and bottom that the warping caused by bending of the tooling would be eliminated.

5. PROPOSED TOOLING CHANGES

Based on the results, the tooling was redesigned. Both the base plate and caul plate were 12.7 mm thick steel, which should eliminate any warping problem caused by the combination of aluminum and steel in the original setup. Steel borders 50.8 mm

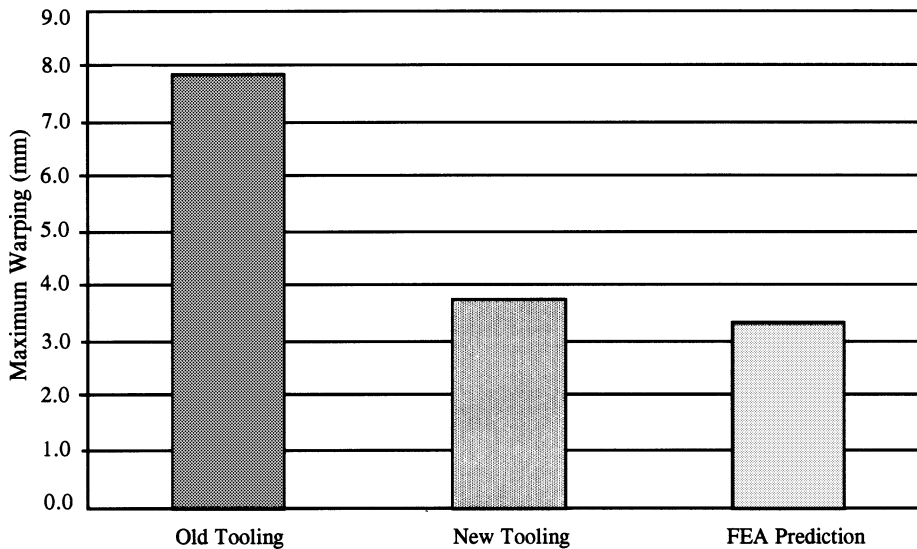


Figure 11. Comparison of warping results.

wide by 12.7 mm thick were rigidly mounted to the base plate with 9.52-mm bolts located about 171.5 mm apart. The borders fit snugly against the mold and completely surround its periphery. The tops of the borders come up to the bottom of each rib. Their purpose was to confine the mold and prevent it from expanding laterally during the cure process. The barrier-frame setup had attempted to do this previously, but since the frames were not anchored to the base plate, they were believed to be too flexible to resist the expansion of the rubber.

An isogrid panel was fabricated without a skin, using the new tooling described above. Leaving off the skin eliminated any warping caused by the rib/skin mismatch, making any improvements secured by the change in tooling easier to judge. A total of 35 tows of IM7/977-2 material were used for the ribs. The tooling was vacuum bagged and cured at 177°C and 0.552 MPa for 2 h. (The entire cure cycle took 20 h, including heat-up and cool-down times.) The resulting ribs-only panel had no detectable warping, as predicted.

Next, an isogrid panel with skin was fabricated using the same tooling. IM7/977-2 material was used for both the skin and the ribs. The ribs were 37 layers of unidirectional tow, and the skin was a six-ply lay-up [+60, -60, 0, 0, -60, +60] of prepreg tape. After bagging, the part was cured at 177°C and 0.552 MPa for 150 min. The 0.552 MPa was applied when the temperature of the composite reached 93.3°C. The part was held for 2 h at that temperature to ensure good resin flow and compaction in the skin and the ribs. The total cure cycle took 16.5 h. The resulting panel had a longitudinal warp of 3.81 mm. This warping was caused by the mismatch in the CTE for the rib and skin. Recall that the predicted value was 3.31 mm and the summary of panel warping is shown in Fig. 11.

6. CONCLUSIONS

Most of the warping in the original isogrid panels was concluded to be the result of differences in the coefficients of thermal expansion of the aluminum, steel, and rubber. A new tooling design, which replaced the aluminum base plate with steel and which rigidly confined the rubber mold between steel borders, eliminated the warping caused by these effects. An unwarped ribs-only panel was successfully made with the new tooling.

The secondary cause of warping was the difference in the thermal expansions of the ribs and skin. A panel with skin was manufactured with the new tooling and found to have a warp of 3.81 mm. A theoretical model developed in the project had predicted a value of 3.3 mm. Further improvements in producing flat panels will depend on finding appropriate materials for the rib/skin and new innovative tooling.

REFERENCES

1. W. Larson and J. Wertz, in: *Space Analysis and Design*, 2nd edn, pp. 421–424. Kluwer Academic Publishers (1992).
2. T. Kim, J. Harvey, J. Koury and J. Tracy, Continuous filament wound isogrid structures for space applications, in: *ASM Conference Proceedings* (1993).
3. T. Kim, Investigation of composite isogrid stiffened structures, in: *Phillips Laboratory Technical Report 95-1112*, pp. 3–7 (1995).
4. A. Reddy and L. Rehfield, Damage tolerance of continuous filament composite isogrid structures: a preliminary assessment, in: *Japan-US Conference Proceedings*, Tokyo, pp. 471–477 (1981).
5. A. Reddy, R. Valisetty and L. Rehfield, Continuous filament wound concepts for aircraft fuselage structures, *J. Aircraft* **22**, 249–255 (1985).
6. L. Rehfield, Continuous filament advanced composite isogrid, AFOSR Contract No. F4962077-C-0077 (1979).
7. C. Moler, in: *The Student Edition of Matlab*, pp. 107–110. Prentice-Hall, Inc., New York (1992).
8. O. Zienkiewicz, in: *The Finite Element Method*, 3rd edn, pp. 325–330. McGraw-Hill, Book Co., New York (1977).
9. S. Tsai, in: *Theory of Composites Design*, pp. 6–13. Think Composites, Dayton (1992).
10. A. Ugural, in: *Stresses in Plates and Shells*, pp. 14–18. McGraw-Hill, Inc., New York (1981).
11. S. Timoshenko and J. Gere, *Theory of Elastic Stability*, 2nd edn. McGraw-Hill, Inc., New York (1981).